Human Molecular Genetics, 2010, Vol. 19, No. 20 **3919–3935**
doi:10.1093/hmg/ddq306
Advance Access published on July 21, 2010

Mitochondrial loss, dysfunction and altered dynamics in Huntington's disease

Jinho Kim[1,2,3], Jennifer P. Moody[1,2,3], Christina K. Edgerly[1], Olivia L. Bordiuk[1], Kerry Cormier[1], Karen Smith[1,2,3], M. Flint Beal[4,5] and Robert J. Ferrante[1,2,3,*]

[1]Geriatric Research Education Clinical Center, New England Veterans Administration VISN 1, Bedford, MA 01730, USA, [2]Department of Neurology, Laboratory Medicine and Pathology and [3]Department of Psychiatry, Boston University School of Medicine, Boston, MA 02118, USA, [4]Department of Neurology and Neuroscience and [5]Department of Neurosurgery, Weill Medical College of Cornell University, New York-Presbyterian Hospital, New York, NY, USA

Received May 10, 2010; Revised and Accepted July 15, 2010

Although a direct causative pathway from the gene mutation to the selective neostriatal neurodegeneration remains unclear in Huntington's disease (HD), one putative pathological mechanism reported to play a prominent role in the pathogenesis of this neurological disorder is mitochondrial dysfunction. We examined mitochondria in preferentially vulnerable striatal calbindin-positive neurons in moderate-to-severe grade HD patients, using antisera against mitochondrial markers of COX2, SOD2 and cytochrome *c*. Combined calbindin and mitochondrial marker immunofluorescence showed a significant and progressive grade-dependent reduction in the number of mitochondria in spiny striatal neurons, with marked alteration in size. Consistent with mitochondrial loss, there was a reduction in COX2 protein levels using western analysis that corresponded with disease severity. In addition, both mitochondrial transcription factor A, a regulator of mtDNA, and peroxisome proliferator-activated receptor-co-activator gamma-1 alpha, a key transcriptional regulator of energy metabolism and mitochondrial biogenesis, were also significantly reduced with increasing disease severity. Abnormalities in mitochondrial dynamics were observed, showing a significant increase in the fission protein Drp1 and a reduction in the expression of the fusion protein mitofusin 1. Lastly, mitochondrial PCR array profiling in HD caudate nucleus specimens showed increased mRNA expression of proteins involved in mitochondrial localization, membrane translocation and polarization and transport that paralleled mitochondrial derangement. These findings reveal that there are both mitochondrial loss and altered mitochondrial morphogenesis with increased mitochondrial fission and reduced fusion in HD. These findings provide further evidence that mitochondrial dysfunction plays a critical role in the pathogenesis of HD.

INTRODUCTION

Huntington's disease (HD) is an autosomal dominant and fatal neurological disorder caused by an expanded trinucleotide CAG repeat in the gene coding for the protein, huntingtin. Although other brain areas are involved, there is selective death of medium-sized spiny striatal projection neurons and depletion of their neurochemical components (1–3). Despite great progress, a direct causative pathway from the HD gene mutation to neuronal dysfunction and death has not yet been established. It has been postulated, however, that mutant huntingtin and its fragments trigger cascades of both impaired and compensatory molecular processes and genetic programs leading to transcriptional dysfunction and mitochondrial damage (4). These pathological pathways ultimately lead to increasingly fragile neurons that are susceptible to more generic stresses, such as oxidative injury, excitotoxic stress, expression of inflammatory signals, pro-apoptotic signals and energy depletion, all of which may play roles in the neuronal death observed in HD (4). Mitochondria are critically vital organelles that generate energy for all molecular processes and regulate cellular function (5). Mitochondrial

*To whom correspondence should be addressed at: GRECC Unit 182B, Bedford VA Medical Center, 200 Springs Road, Bedford, MA 01730, USA. Tel: +1 7816872908; Fax: +1 7816873515; Email: rjferr@bu.edu

energy production is essential to carry out vital cellular processes, such as neurotransmitter release and reuptake. Neurons are especially vulnerable to mitochondrial abnormalities, as they have a high metabolic demand and extraordinary energy requirements (6). Mitochondrial impairment leads to increased production of reactive oxygen species and plays a central role in both necrotic and apoptotic cell death. There is strong evidence that mitochondrial dysfunction plays a prominent role in the pathogenesis of HD (7–10).

Evidence for mitochondrial abnormalities in HD was first observed over three decades ago in ultrastructural studies on brain biopsies of HD patients (11). Consistent with these findings, electron transport chain complex subunits have been reported to be involved in the selective degeneration of the basal ganglia (12,13) and, as such, it is not unreasonable to suggest that the genetic HD mutation may alter nuclear-encoded components of electron transport complexes, resulting in primary mitochondrial dysfunction. In fact, significant reductions have been reported in mitochondrial complex I, II–III and IV activities in the neostriatum from HD patients that are not present in other brain regions (10,14–20), although these abnormalities are not observed in premanifest and early-stage HD patients (21). It is of interest to note, however, that in patients with other trinucleotide repeat diseases, such as spinocerebellar ataxias, mitochondrial abnormalities and metabolic defects are present, linking mitochondrial dysfunction as a common mechanism to neurodegenerative diseases caused by polyglutamine gene mutations (22,23).

Mutant htt protein induces abnormal transcriptional regulation of TATA-binding proteins and Sp1, resulting in transcriptional dysregulation of nuclear-encoded mitochondrial genes in HD (24). Support for this comes from studies showing that the transcriptional repression of peroxisome proliferator-activated receptor-co-activator gamma-1 alpha (PGC-1α), a key regulator of mitochondrial energy metabolism and mitochondrial gene expression (25,26), is selectively decreased in the caudate nucleus from premanifest HD patients (27). Recent evidence shows that, in both muscle biopsies and myoblast cultures from HD subjects, there are significant reductions in PGC-1α and mitochondrial transcription factor A (TFAM), a nuclear-encoded mitochondrial transcription factor (28). Abnormal PGC-1α function results in significant mitochondrial impairment. In addition, several studies have showed mitochondrial trafficking abnormalities in HD in which defective mitochondrial transport results in neuronal death (29,30). In this circumstance, mutant huntingtin sequesters constituent parts of the mitochondrial machinery in HD patients (29).

Lastly, there is evidence from experimental models that mitochondrial fission and fusion may be altered in HD, leading to neuronal death (30–33). Mitochondria are morphologically dynamic organelles that are distributed throughout the cell by fission and fusion to form individual units or interconnected networks (34). In normal healthy cells, there is equilibrium between these two opposing states of organelle fusion and fission (35,36). Modulation of both mitochondrial shape and size provides a mechanism for mitochondrial trafficking in positioning mitochondria throughout the cell. The primary proteins controlling mitochondrial fission include dynamin-related protein (Drp1) (37–39) and mitochondrial fission 1 (Fis1) (39–41), along with a number of other regulatory proteins (39). Mitochondrial fusion is controlled by homologs of Fzo (fuzzy onions)1p, a large GTPase of the outer mitochondrial membrane, and includes the mitofusins (Mfn) 1 and 2, in addition to an inner-membrane-localized, dynamin-related protein, OPA1 (39). There is evidence to suggest that mutant huntingtin physically impairs mitochondrial mobility and trafficking (30). Although increasing polyglutamine repeats result in greater mitochondrial fragmentation and reduced ATP levels, suppression of fission and promotion of fusion ameliorate mitochondrial fission, augment ATP levels and attenuate cell death in HeLa cells expressing expanded polyglutamine proteins (32).

Although mitochondrial dysfunction has been reported both in animal models of HD and in HD patients, there are no studies that examine the progressive loss of mitochondria along with altered mitochondrial fission and fusion dynamics in HD patients. As such, we performed quantitative analyses of mitochondria identified using immunohistochemical staining for Mt-COX2, superoxide dismutase 2 (SOD2) and cytochrome *c* in striatal calbindin-immunoreactive neurons, which are preferentially vulnerable in HD. We also correlated the findings with Mt-COX2, PGC-1α and TFAM protein levels assessed using western analysis. In parallel, we investigated alterations in mitochondrial fission and fusion dynamics and their respective proteins, along with mitochondrial PCR array expression profiling to characterize corresponding changes in mitochondrial function.

RESULTS

Using 3D deconvolutional digital imaging, combined immunofluorescence of calbindin antisera and Mt-COX2 antisera in tissue sections from moderate Grade 2 HD and very severe Grade 4 HD patients showed a grade-dependent reduction in the number of mitochondria in HD, compared with age-matched control subjects (Fig. 1A). Quantitative analysis revealed a significant reduction in the density of perikaryal mitochondria in medium-sized calbindin spiny striatal neurons from both Grade 2 and Grade 4 HD patients (control patients $1.31 \pm 0.09\ \mu m^3$; Grade 2 HD patients $0.85 \pm 0.19\ \mu m^3$, $P < 0.0001$; Grade 4 HD patients $0.48 \pm 0.16\ \mu m^3$, $P < 0.00002$). In addition, there was a significant difference between Grade 2 and Grade 4 HD patients ($P < 0.01$). Despite progressive neuronal atrophy associated with increased disease severity, these data represent a 35 and 66% loss in mitochondria from Grade 2 and Grade 4 HD patients, respectively. In addition to the observed mitochondrial loss, further analysis of the size of mitochondria showed that with the progression of disease severity there were marked alterations in the distribution of the size of very small, small, medium and large mitochondria (Fig. 1B). Mitochondria binned according to size resulted in four distinct peaks, with the largest number within very small ($0.18\ \mu m^3$) and small ($0.26\ \mu m^3$) mitochondria, in comparison with medium ($0.32\ \mu m^3$) and large ($0.4\ \mu m^3$) mitochondria. These peak sizes remained constant in control and HD patients. Although there was a progressive loss of mitochondria in HD patients, there was a greater loss of

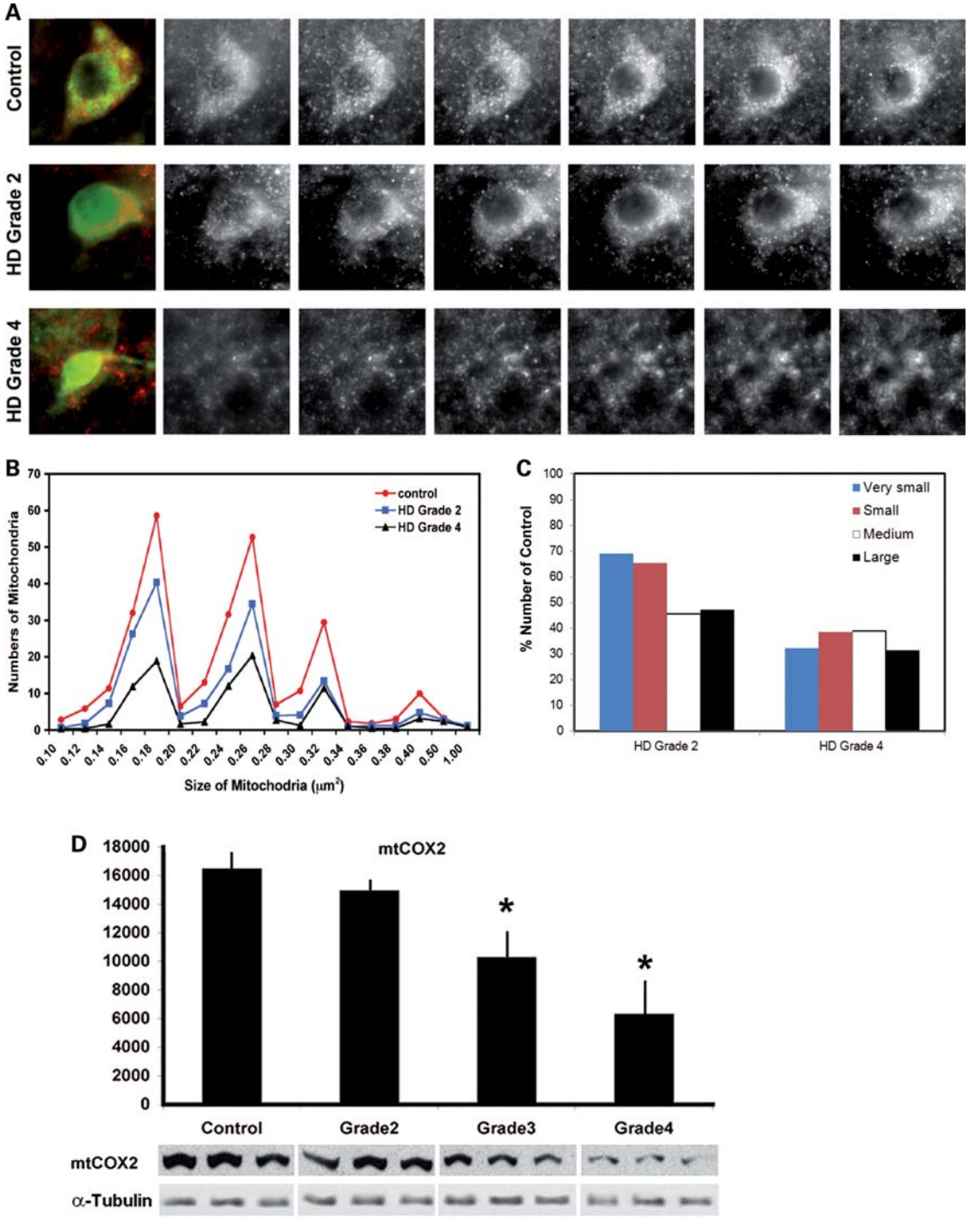

Figure 1. 3D deconvolutional digital imaging using combined immunofluorescence of calbindin antisera identifying medium-sized spiny caudate neurons and COX2 antisera marking mitochondria from moderate Grade 2 HD and very severe Grade 4 HD patients, compared with an age-matched control subject (**A**). The first panel from each row represents a color image through the stacked images. Green denotes calbindin reactivity and red denotes Mt-COX2. The successive black and white panels within each row represent serial step sections through the identified neuron showing the density of mitochondrial immunostaining. Compared with the age-matched normal control, there was a significant loss of mitochondria in moderate Grade 2 HD that becomes markedly apparent in severe Grade 4 HD sections. (**B**) The graph represents quantitative mitochondrial binning according to size that resulted in four peaks observed in control and HD specimens. There was a progressive loss of mitochondria in HD patients. (**C**) The graph represents the percentile difference in mitochondrial size, as related to Grade 2 and Grade 4 HD. Consistent with the findings of COX2-positive mitochondrial loss, western analysis of brain lysates of the medial caudate nucleus in Grades 2, 3 and 4 from HD patients and age-matched control subjects showed a grade-dependent loss of COX2-immunoreactivity (**D**). Representative western gels of COX2 and alpha tubulin activities are present under each bar in the graph. An asterisk represents significance.

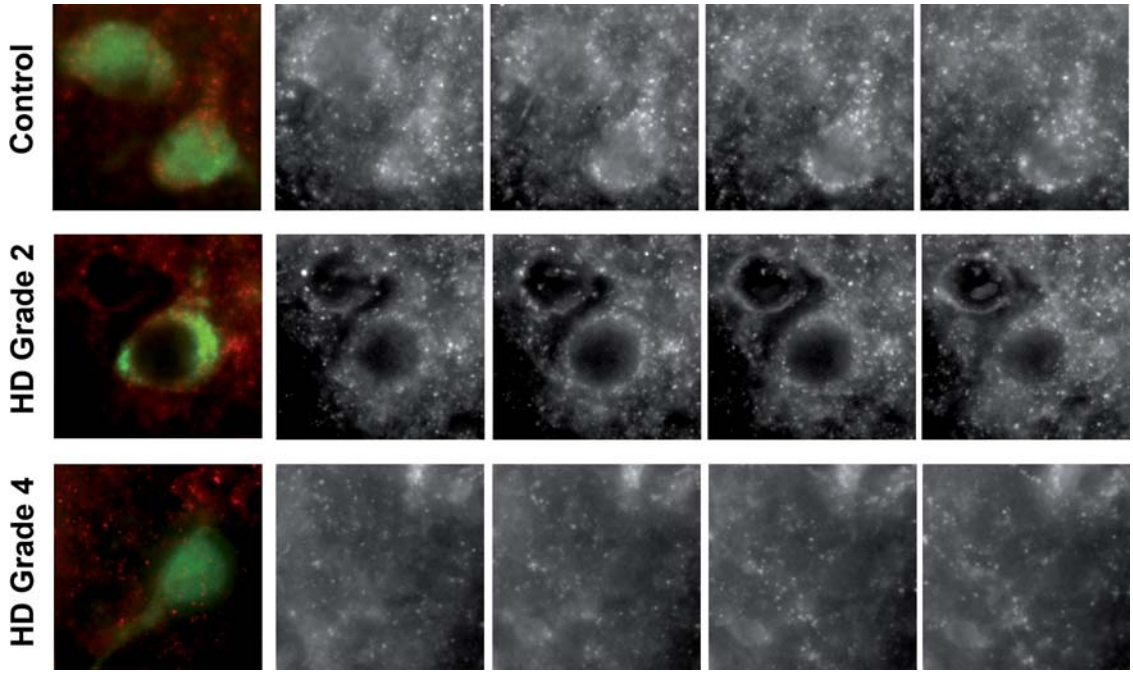

Figure 2. 3D deconvolutional digital imaging of combined immunofluorescence of calbindin antisera identifying medium-sized spiny caudate neurons and SOD2 antisera marking mitochondria from moderate Grade 2 HD and very severe Grade 4 HD patients, compared with an age-matched control subject. Consistent with the combined calbindin/COX2 results, there was a significant loss of mitochondria in moderate Grade 2 HD, with a greater loss of mitochondria in the severe Grade 4 HD sections.

medium- (54%) and large-sized (55%) mitochondria in early manifest disease (Grade 2), with very little or no change in late-stage (Grade 4) disease. In contrast, the loss of very small and small mitochondria in Grade 2 HD was much less at 38 and 35%, respectively, with the greatest loss of very small and small mitochondria occurring in Grade 4 HD patients, 68 and 62%, respectively (Fig. 1C).

Consistent with the findings of COX2-positive mitochondrial loss, western analysis of brain lysates of the medial caudate nucleus in Grades 2, 3 and 4 from HD patients and age-matched control subjects showed a grade-dependent loss of COX2-immunoreactivity (Fig. 1D). Although there was a 10% loss of COX2 immunoreactivity in Grade 2 HD patients, this did not reach significance. Significant losses were observed, however, in Grade 3 HD ($P < 0.01$) and Grade 4 HD ($P < 0.004$) patients, with a 38 and 62% reduction, respectively, in immunoreactivity.

Comparable with the Mt-COX2 findings, stacked images from combined calbindin and SOD2 immunofluorescence showed similar findings, with a progressive marked reduction in SOD2-positive mitochondrial density in medium-sized calbindin-positive neurons in HD patients (Fig. 2). Quantitative analysis showed a significant reduction in overall mitochondrial density in Grade 2 HD patients (31%), with a more marked loss of mitochondria in Grade 4 HD patients (62%) (control patients $0.42 \pm 0.8\ \mu m^3$; Grade 2 HD patients $0.29 \pm 0.6\ \mu m^3$, $P < 0.001$; Grade 4 HD patients $0.16 \pm 0.5\ \mu m^3$, $P < 0.0001$). In comparison with the COX2 data, the overall density of SOD2-positive mitochondria was ~3-fold less, suggesting that SOD2-positive mitochondria may represent a distinct subset. In addition, there was a significantly greater decrease in mitochondrial density in Grade 4 patients, in comparison with Grade 3 patients ($P < 0.01$).

Qualitative confirmation of both the mitochondrial COX2 and SOD2 data was made using a third mitochondrial marker, cytochrome *c*. As in the COX2 and SOD2 findings in Figures 1 and 2, mitochondrial density was reduced in HD patients and worsened with increasing severity of disease (Fig. 3).

Proteins which are regulators of mitochondrial function and biogenesis, and activators of mitochondrial gene expression, include PGC-1α (25,26) and TFAM (42). Both proteins have been reported to be reduced in HD (27,28). There is a significant decrease in PGC-1α mRNA in the caudate nucleus in premanifest HD patients (27). This downregulation is accompanied by reduced expression of genes involved in energy metabolism. PGC-1α and TFAM are also reduced in muscle biopsies and myoblast cultures from HD subjects (28). We confirmed and extended these findings by examining levels of PGC-1α and TFAM in relation to the progression of HD. Western analysis showed that there were significant grade-dependent reductions in both PGC-1α and TFAM in brain lysates from HD patients (Fig. 4). PGC-1α immunoreactivity was decreased by 16% in Grade 2 HD ($P < 0.042$), 39% in Grade 3 HD ($P < 0.013$) and 70% in Grade 4 HD ($P < 0.001$) specimens. Similar grade-dependent reductions were found in western analyses of TFAM, with a 15% decrease in Grade 2 HD ($P < 0.01$), 32% in Grade 3 HD ($P < 0.0018$) and 41% in Grade 4 HD ($P < 0.0006$) specimens. Although our findings may correlate with neuronal loss, the fact that there is a significant 30% loss of PGC-1α in premanifest disease (27) suggests that the loss of PGC-1α is not an epiphenomenon.

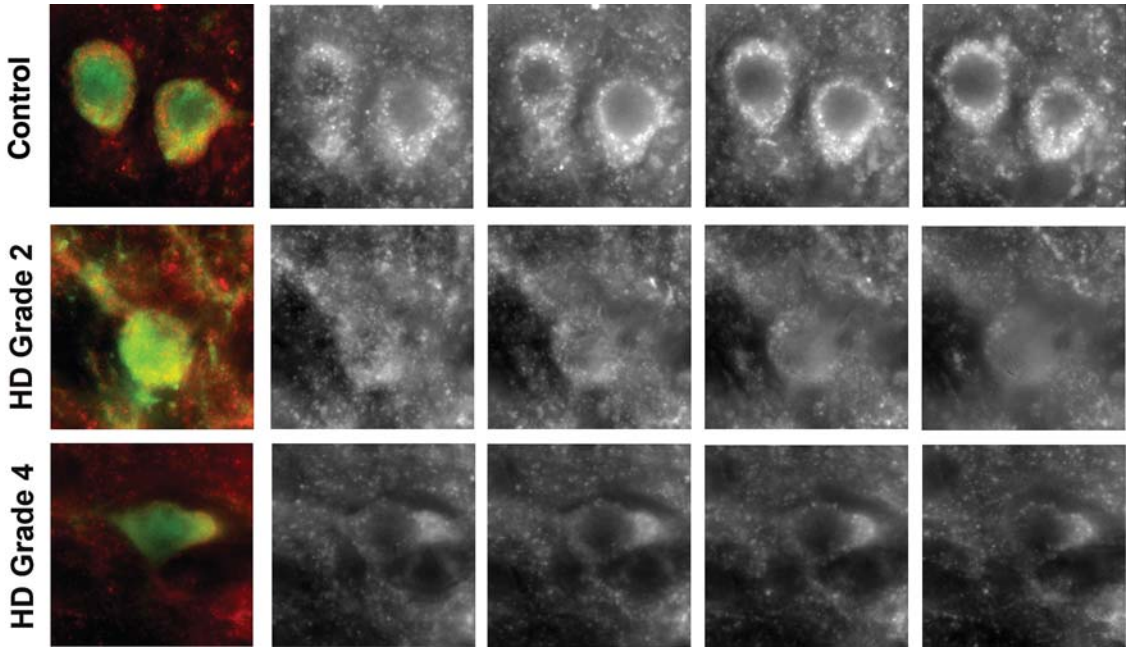

Figure 3. Cytochrome *c* mitochondrial immunoactivity in HD caudate nucleus. 3D deconvolutional digital imaging of combined immunofluorescence of calbindin antisera identifying medium-sized spiny caudate neurons and cytochrome *c* antisera marking mitochondria from moderate Grade 2 HD and very severe Grade 4 HD patients, compared with an age-matched control subject. The loss of mitochondria confirmed the findings observed in the COX2 and SOD2 studies.

Large cholinergic striatal neurons are relatively spared in HD patients (1). Consistent with this finding and of great interest, there was no significant difference in COX2-positive mitochondrial density in large cholinergic neurons within the medial caudate nucleus from HD patients, compared with age-matched control patients (control patients: $1.62 \pm 0.15\ \mu m^3$; Grade 2 HD patients $1.49 \pm 0.17\ \mu m^3$, $P < 0.33$; Grade 4 HD patients $1.41 \pm 0.20\ \mu m^3$, $P < 0.28$) (Fig. 5).

We have obtained novel evidence which suggests that altered mitochondrial dynamics, a pathophysiological process that results in bioenergetic dysfunction and subsequent neuronal cell death, is drastically altered in HD patients. Immunoreactive markers of mitochondrial fission (Drp1) and fusion (Mfn1) proteins were markedly changed in striatal human HD tissue sections, compared with age-matched control subjects. Histopathology of Drp1 showed a progressive increased protein expression in both Grade 2 and Grade 4 HD specimens, whereas Mfn1 immunoreactivity was increased in Grade 2 HD specimens with a subsequent reduction in Grade 4 HD (Fig. 6). Western analysis of both proteins in brain tissue lysates from Grades 2, 3 and 4 HD frozen specimens was consistent with the immunohistology data (Fig. 6). There was a significant grade-dependent increase in Drp1 protein levels, with a 23% increase in Grade 2 HD ($P < 0.032$), 50% increase in Grade 3 HD ($P < 0.014$) and a 59% increase in Grade 4 HD ($P < 0.0015$) specimens. In contrast, although there was an initial upregulation of Mfn1 by 42% in Grade 2 HD tissue lysates ($P < 0.001$), there was a significant subsequent reduction in Mfn1 protein by 60% in Grade 3 HD ($P < 0.0004$) and by 70% in Grade 4 HD ($P < 0.0008$) specimens. It is of interest to note that the levels of Drp1 and Mfn1 in control specimens, as measured from western analyses, were not significantly different, confirming previous studies that both fission and fusion of mitochondria are at equilibrium under normal conditions (35,36). These findings are consistent with the hypothesis that mitochondrial dynamics are disrupted in HD (31,33).

Mitochondrial PCR array expression profiling was performed in caudate nucleus striatal tissue samples from Grades 2, 3 and 4 HD patients and age-matched control subjects. The 84 mitochondrial-gene probe set showed changes in both upregulation and downregulation of mitochondrial genes, with an overall ratio of 9.3:1 in gene upregulation from all HD grades of severity. There was an increased expression in mitochondrial genes from 24.5% in Grade 2 HD, with the greatest changes occurring in Grade 3 HD specimens at 56%, and a subsequent falloff in overall gene expression change in Grade 4 HD specimens to 19.5%. A complete listing of the mitochondrial gene expression levels can be found in Table 1. The gene changes from Grades 2, 3 and 4 HD patients are shown graphically in scatter plots (Fig. 7). The genes monitored by the mitochondria PCR array include regulators and mediators of mitochondrial molecular transport of not only metabolites needed for the electron transport chain and oxidative phosphorylation, but also of the ions required for maintaining mitochondrial membrane polarization and potential that are critical for ATP synthesis. This array's gene profiling also targets previously translated and folded proteins which localize into the outer and inner mitochondrial membranes, as well as into the mitochondrial matrix. In addition, the intrinsic apoptosis pathway genes activated by intracellular damage signaling are also represented

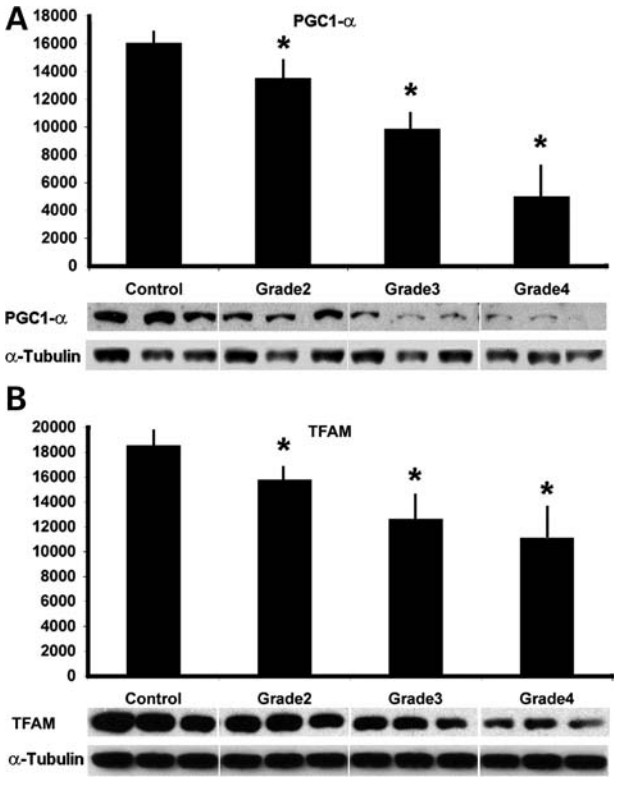

Figure 4. Western analysis of the caudate nucleus in Grades 2, 3 and 4 from HD patients showing significant grade-dependent reductions in both PGC-1α (**A**) and TFAM (**B**) in brain lysates from HD patients. Representative western gels of PGC-1α, TFAM and alpha tubulin activities are present under each bar in the graph. An asterisk represents significance.

on this array. The PCR array data findings from our studies show largely upregulated gene expression and to some degree reflect impairment and compensatory mechanisms.

There were 10 mRNA changes associated with downregulation, with a ≥2-fold decrease in expression, most of which were found in severe and very severe HD specimens (Table 1). These decreases included stratifin (*SFN*), apoptosis-inducing factor mitochondrion-associated 2 (*AFIM2*), neurofilament light polypeptide (*NEFL*), translocase of inner mitochondrial membrane 50 homolog (*TIMM50*), translocase of outer mitochondrial membrane 70 homolog A (*TOMM70A*), translocase of outer mitochondrial membrane 34 (*TOMM34*), heat shock protein 90 kDa alpha (cytosolic) class A member (*HSP90AA1*) and three solute mitochondrial carrier family 25 genes (*SLC25A31*, adenine nucleotide translocator; *SLC25A27*; and *SLC25A23*, phosphate carrier).

There were 57 mRNA upregulated changes in HD patients in which there was a ≥2-fold increase in expression, with many of these mRNA changes present across Grades 2, 3 and 4 (Table 1). We focused on the most robust changes in which there was a ≥4-fold change (19 mRNAs), reaching as high as 38-fold. Among the mRNAs in HD patients meeting these inclusion criteria were tumor protein p53 (*TP53*), *SOD2*, *SFN*, BCL2-like 1 (*BCL2L1*), *BAK1*, translocase of inner mitochondrial membrane 44 homolog (*TIMM44*), translocase of inner mitochondrial membrane 17 homolog B (*TIMM17B*), tafazzin (*TAZ*), fracture callus 1 homolog (*FXC1*), translocase of outer mitochondrial membrane 40 homolog (*TOMM40*), uncoupling protein 3 (mitochondrial, proton carrier) (*UCP3*), StAR-related lipid transfer (*START*) domain containing 3 (*STARD3*) and seven solute mitochondrial carrier family 25 genes (*SLC25A37*; *SLC25A25*, phosphate carrier; *SLC25A20*, carnitine/acylcarnitine translocase; *SLC25A2*, ornithine transporter; *SLC25A17*, peroxisomal membrane protein, 34 kDa; *SLC25A13*, citrin; and *SLC25A1*, citrate transporter member 1).

The PCR array data associated with mitochondrial fission and fusion reflected the western analysis findings. There was a grade-dependent increase in mRNA for the fission protein (*DNM1L/DRP1*), with the highest expression in Grade 4 HD tissue specimens. In addition, early overexpression of fusion genes (*MFN1* and *MFN2*) was present, with a continued reduction in gene expression with greater disease severity.

DISCUSSION

Herein, we show that quantitative analyses of the number of perikaryal mitochondria, identified by multiple immunohistochemical markers including COX2, SOD2 and cytochrome *c* in vulnerable striatal calbindin-positive neurons from HD patients, were reduced with increasing severity of disease, although significant mitochondrial loss was not found in the relatively spared large cholinergic striatal neurons. In addition, western analysis of brain lysates from the caudate nucleus revealed a grade-dependent loss of Mt-COX2 activity, with similar findings in the transcriptional co-activators of mitochondrial gene expression and biogenesis, PGC-1α and TFAM. In parallel, we found significant morphological and biochemical alterations in mitochondrial fission and fusion, as assessed by mitochondrial size, and their respective proteins, Drp1 and Mfn1. Consistent with the above alterations showing mitochondrial abnormalities in HD patients, mitochondrial PCR array expression profiling identified a large number of corresponding changes in genes associated with membrane potential, mitochondrial transport and localization, inner and outer membrane translocation and apoptosis.

Mitochondria are crucial power-producing organelles that provide most of the cellular ATP through oxidative phosphorylation, exhibit highly dynamic structural and functional diversity and play a significant role in neuronal life and death. Neurons are metabolically active cells with a high energy requirement and, as such, mitochondrial dysfunction results in a cascade of events that include reduced ATP production, altered calcium homeostasis, increased reactive oxygen species, apoptosis and cytochrome *c* release that subsequently lead to neuronal death (32,43). Several lines of evidence lend support to the hypothesis that mitochondrial impairment and energy disturbance are an important part of the pathophysiological process in neurodegenerative disorders, particularly in HD (7,44). There is substantial evidence from experimental models of HD that suggests an important role of mitochondrial dysfunction in the pathogenesis of HD (7,10,45). In R6/2 HD mice, there is a significant reduction in striatal aconitase activity and a decrease of mitochondrial complex IV activities in both the striatum and neocortex

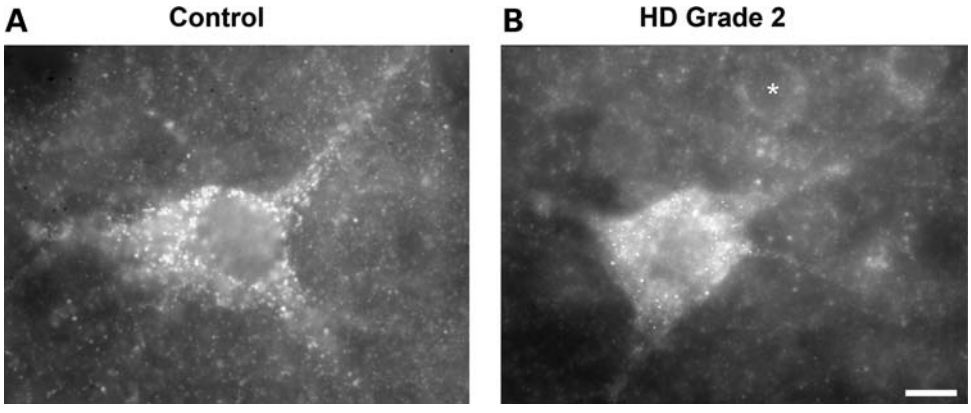

Figure 5. COX2-positive mitochondrial density in large cholinergic neurons within the HD neostriatum, compared with age-matched control caudate nucleus. (**A** and **B**) The images represent black and white 3D stacked images of a large striatal neuron in control caudate nucleus (A) and Grade 4 HD caudate nucleus (B). Mt-COX2-positive immunoreactive mitochondria are identified by white spheroid profiles. Asterisk shows a medium-sized striatal neuron for comparison. The bar in B represents 20 μm.

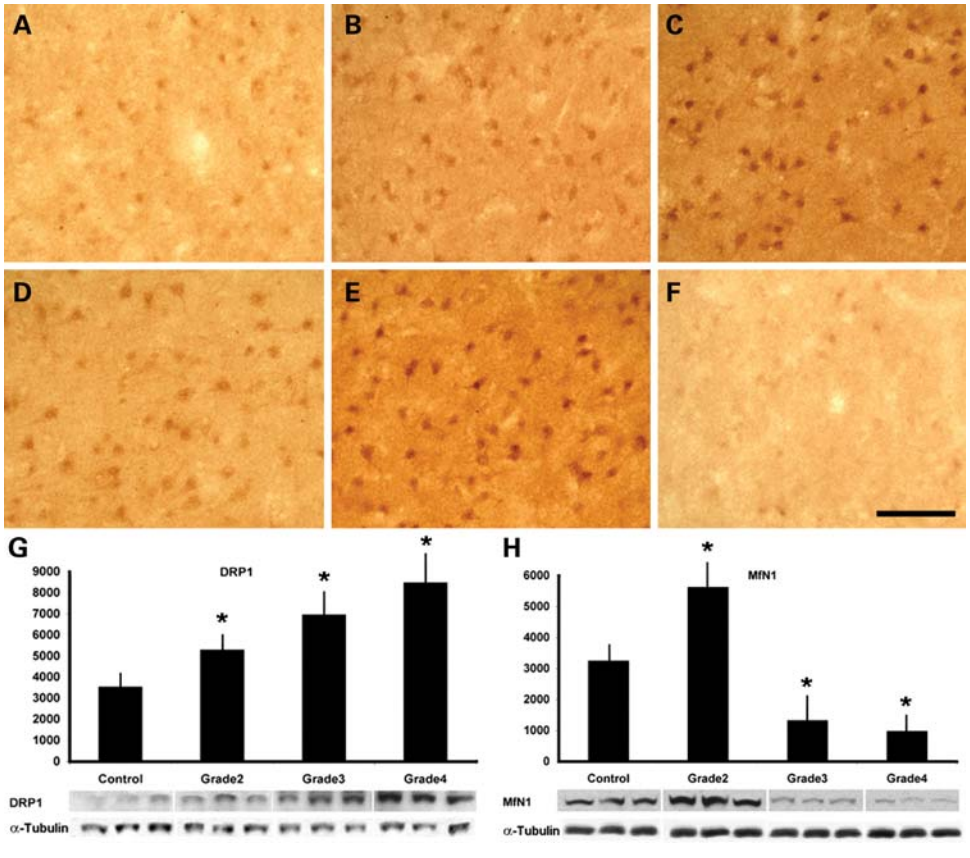

Figure 6. Histopathology and western analysis of Drp1 and Mfn1 activities. Immunohistochemistry of Drp1activity in the medial caudate nucleus showed a progressive increase in protein expression in Grade 2 (**B**) and Grade 4 (**C**) HD specimens, compared with a normal control patient (**A**). Greater immunoreactivity is observed in both neurons and in the neuropil. Mfn1 immunoreactivity was markedly increased in Grade 2 (**E**) HD caudate nucleus, with a significant reduction in Grade 4 (**F**) specimens, compared with a normal control (**D**). Western analysis findings paralleled the immunohistology observations characterizing both proteins in brain tissue lysate from Grades 2, 3 and 4 HD frozen specimens (**G**, Drp1 and **H**, Mfn1). The bar in F represents 100 μm. An asterisk denotes significance.

(46). In addition, the mitochondrial ubiquinone, coenzyme Q_{10}, is significantly reduced in R6/2 mice (47). There is an age-dependent decrease in the relative amplification of mtDNA from both the striatum and cerebral cortex in R6/2 mice (48). Mitochondria from both R6/2 mice and YAC128 mice show increased Ca^{2+}-loading capacity, whereas challenged neurons from full-length Hdh150 knock-in heterozygote mice are more vulnerable to Ca^{2+} deregulation (49).

Table 1. PCR array profiling in HD caudate nucleus specimens

Related functions	Symbol	RefSeq	Description	Grade 2 HD/control (fold up- or downregulation)	Grade 3 HD/control (fold up- or downregulation)	Grade 4 HD/control (fold up- or downregulation)
Membrane polarization and potential	*BAK1*	NM_001188	BCL2-antagonist/killer 1	9.06	4.4	2.26
	BCL2	NM_000633	B-cell CLL/lymphoma 2	1.22	2.23	−1
	BCL2L1	NM_138578	BCL2-like 1	5.43	4.68	4.88
	TP53	NM_000546	Tumor protein p53	2.85	5.38	7.55
	UCP1	NM_021833	Uncoupling protein 1 (mitochondrial, proton carrier)	3.27	1.4	−1.37
	UCP3	NM_003356	Uncoupling protein 3 (mitochondrial, proton carrier)	10.41	38.27	8.98
Mitochondrial transport	*AIP*	NM_003977	Aryl hydrocarbon receptor interacting protein	2.68	2.53	2.82
	BAK1	NM_001188	BCL2-antagonist/killer 1	9.06	4.4	2.26
	BCL2	NM_000633	B-cell CLL/lymphoma 2	1.22	2.23	−1
	BCL2L1	NM_138578	BCL2-like 1	5.43	4.68	4.88
	FXC1	NM_012192	Fracture callus 1 homolog (rat)	3.92	7.3	2.9
	HSP90AA1	NM_001017963	Heat shock protein 90 kDa alpha (cytosolic), class A member 1	−1.02	3.13	−2.01
	HSPD1	NM_002156	Heat shock 60 kDa protein 1 (chaperonin)	1.24	3.09	2.23
	IMMP2L	NM_032549	IMP2 inner mitochondrial membrane peptidase-like (*Saccharomyces cerevisiae*)	1.71	2.41	2.56
	MFN2	NM_014874	Mitofusin 2	2.01	1.1	1.07
	MIPEP	NM_005932	Mitochondrial intermediate peptidase	2.03	2.39	2.94
	MTX2	NM_006554	Metaxin 2	−1.39	1.05	−1.15
	STARD3	NM_006804	StAR-related lipid transfer (START) domain containing 3	18.25	12.19	7.81
	TP53	NM_000546	Tumor protein p53	2.85	5.38	7.55
	TSPO	NM_000714	Translocator protein (18 kDa)	1.19	1.42	2.44
	UCP1	NM_021833	Uncoupling protein 1 (mitochondrial, proton carrier)	3.27	1.4	−1.37
	UCP3	NM_003356	Uncoupling protein 3 (mitochondrial, proton carrier)	10.41	38.27	8.98
Small molecule transport	*SLC25A1*	NM_005984	Solute carrier family 25 (mitochondrial carrier; citrate transporter), member 1	4.32	4.08	3.17
	SLC25A10	NM_012140	Solute carrier family 25 (mitochondrial carrier; dicarboxylate transporter), member 10	2.22	1.02	−1.02
	SLC25A13	NM_014251	Solute carrier family 25, member 13 (citrin)	3.71	5.46	8.2
	SLC25A17	NM_006358	Solute carrier family 25 (mitochondrial carrier; peroxisomal membrane protein, 34 kDa), member 17	2.16	4.28	4.65
	SLC25A2	NM_031947	Solute carrier family 25 (mitochondrial carrier; ornithine transporter) member 2	5.46	21.98	−1.05
	SLC25A20	NM_000387	Solute carrier family 25 (carnitine/acylcarnitine translocase), member 20	4.44	3.68	2.36
	SLC25A23	NM_024103	Solute carrier family 25 (mitochondrial carrier; phosphate carrier), member 23	−1.23	−4.9	−7.7
	SLC25A24	NM_013386	Solute carrier family 25 (mitochondrial carrier; phosphate carrier), member 24	−1.59	2.19	−1.04
	SLC25A25	NM_052901	Solute carrier family 25 (mitochondrial carrier; phosphate carrier), member 25	1.56	4.65	2.49
	SLC25A27	NM_004277	Solute carrier family 25, member 27	−2.16	−1.72	−2.63
	SLC25A31	NM_031291	Solute carrier family 25 (mitochondrial carrier; adenine nucleotide translocator), member 31	−5.17	2.58	−1.67
	SLC25A37	NM_016612	Solute carrier family 25, member 37	2.87	5.65	4.58

Targeting proteins to mitochondria	*AIP*	NM_003977	Aryl hydrocarbon receptor interacting protein	2.68	2.53	2.82
	FXC1	NM_012192	Fracture callus 1 homolog (rat)	3.92	7.3	2.9
	HSPD1	NM_002156	Heat shock 60 kDa protein 1 (chaperonin)	1.24	3.09	2.23
	IMMP2L	NM_032549	IMP2 inner mitochondrial membrane peptidase-like (*S. cerevisiae*)	1.71	2.41	2.56
	MFN1	NM_033540	Mitofusin 1	2.58	1.6	−1.1
	MIPEP	NM_005932	Mitochondrial intermediate peptidase	2.03	2.39	2.94
	TSPO	NM_000714	Translocator protein (18 kDa)	1.19	1.42	2.44
Mitochondrion protein import	*AIP*	NM_003977	Aryl hydrocarbon receptor interacting protein	2.68	2.53	2.82
	COX10	NM_001303	COX10 homolog, cytochrome c oxidase assembly protein, heme A: farnesyltransferase (yeast)	1.3	−1.04	−1.58
	COX18	NM_173827	COX18 cytochrome *c* oxidase assembly homolog (*S. cerevisiae*)	2.85	1.25	1.48
	DNAJC19	NM_145261	DnaJ (Hsp40) homolog, subfamily C, member 19	−1.06	−1.22	−1.13
	FXC1	NM_012192	Fracture callus 1 homolog (rat)	3.92	7.3	2.9
	HSPD1	NM_002156	Heat shock 60 kDa protein 1 (chaperonin)	1.24	3.09	2.23
	MIPEP	NM_005932	Mitochondrial intermediate peptidase	2.03	2.39	2.94
	SH3GLB1	NM_016009	SH3-domain GRB2-like endophilin B1	1.21	2.34	1.55
Outer membrane translocation	*TOMM34*	NM_006809	Translocase of outer mitochondrial membrane 34	−1.43	−3.16	−3.93
	TOMM40	NM_006114	Translocase of outer mitochondrial membrane 40 homolog (yeast)	9.78	34.73	2.69
	TOMM70A	NM_014820	Translocase of outer mitochondrial membrane 70 homolog A (*S. cerevisiae*)	−1.84	−3.59	−4.58
Inner membrane translocation	*FXC1*	NM_012192	Fracture callus 1 homolog (rat)	3.92	7.3	2.9
	IMMP2L	NM_032549	IMP2 inner mitochondrial membrane peptidase-like (*S. cerevisiae*)	1.71	2.41	2.56
	TAZ	NM_000116	Tafazzin	3.39	7.99	5.16
	TIMM10	NM_012456	Translocase of inner mitochondrial membrane 10 homolog (yeast)	2.87	1.2	1.27
	TIMM17B	NM_005834	Translocase of inner mitochondrial membrane 17 homolog B (yeast)	2.16	4.25	1.63
	TIMM44	NM_006351	Translocase of inner mitochondrial membrane 44 homolog (yeast)	1.93	18.87	−1.09
	TIMM50	NM_001001563	Translocase of inner mitochondrial membrane 50 homolog (*S. cerevisiae*)	1.43	−2.3	−1.24
Mitochondrial fission and fusion	*COX18*	NM_173827	COX18 cytochrome *c* oxidase assembly homolog (*S. cerevisiae*)	2.85	1.25	1.48
	FIS1	NM_016068	Fission 1 (mitochondrial outer membrane) homolog (*S. cerevisiae*)	2.23	2.25	1.68
	MFN1	NM_033540	Mitofusin 1	2.58	1.6	−1.1
	DNM1L	NM_005690	Dynamin 1-like	1.16	1.96	2.34
	MFN2	NM_014874	Mitofusin 2	2.01	1.1	1.07
	OPA1	NM_130837	Optic atrophy 1 (autosomal dominant)	1.14	−1.1	−1.11

Continued

Table 1. *Continued*

Related functions	Symbol	RefSeq	Description	Grade 2 HD/control (fold up- or downregulation)	Grade 3 HD/control (fold up- or downregulation)	Grade 4 HD/control (fold up- or downregulation)
Mitochondrial localization apoptotic genes	*NEFL*	NM_006158	Neurofilament, light polypeptide	−3.48	−13.76	−8.72
	RHOT2	NM_018307	Ras homolog gene family, member T1	2.6	1.86	1.2
	AIFM2	NM_032797	Apoptosis-inducing factor, mitochondrion-associated, 2	−1	−1.01	−2.12
	BAK1	NM_001188	BCL2-antagonist/killer 1	9.06	4.4	2.26
	BBC3	NM_014417	BCL2-binding component 3	3.43	3.7	1.95
	BCL2	NM_000633	B-cell CLL/lymphoma 2	1.22	2.23	−1
	BCL2L1	NM_138578	BCL2-like 1	5.43	4.68	4.88
	CDKN2A	NM_000077	Cyclin-dependent kinase inhibitor 2A (melanoma, p16, inhibits CDK4)	3.89	2.43	−1.08
	DNM1L	NM_005690	Dynamin 1-like	1.16	1.96	2.34
	SFN	NM_006142	Stratifin	1.13	8.74	−3.06
	SH3GLB1	NM_016009	SH3-domain GRB2-like endophilin B1	1.21	2.34	1.55
	SOD2	NM_000636	Superoxide dismutase 2, mitochondrial	4.5	7.51	1.58
	TP53	NM_000546	Tumor protein p53	2.85	5.38	7.55
Housekeeping gene	*RPL13A*	NM_012423	Ribosomal protein L13a	2.51	1.31	1.24

The mRNA changes are categorized by mitochondrial function.

Figure 7. Scatter plots of gene changes from Grade 2 (**A**), Grade 3 (**B**) and Grade 4 (**C**) HD patients. The center black-line represents the cipher, and upregulation and downregulation are noted by the red and green arrows, respectively. One- to 2-fold (dark gray zone) and 2- to 4-fold (light gray zone) mRNA changes are represented on both sides of each figure. Downregulated mRNA changes ≥2-fold included stratifin (*SFN*), apoptosis-inducing factor mitochondrion-associated 2 (*AFIM2*), neurofilament light polypeptide (*NEFL*), translocase of inner mitochondrial membrane 50 homolog, translocase of outer mitochondrial membrane 70 homolog A (*TOMM70A*), translocase of outer mitochondrial membrane 34 (*TOMM34*), heat shock protein 90 kDa alpha (cytosolic) class A member (*HSP90AA1*) and three solute mitochondrial carrier family 25 genes (*SLC25A31*, adenine nucleotide translocator; *SLC25A27*; and *SLC25A23*, phosphate carrier). Those upregulated mRNA changes ≥4-fold are identified as tumor protein p53 (*TP53*), superoxide dismutase 2 (*SOD2*), stratifin (*SFN*), BCL2-like 1 (*BCL2L1*), *BAK1*, translocase of inner mitochondrial membrane 44 homolog (*TIMM44*), translocase of inner mitochondrial membrane 17 homolog B (*TIMM17B*), tafazzin (*TAZ*), fracture callus 1 homolog (*FXC1*), translocase of outer mitochondrial membrane 40 homolog (*TOMM40*), uncoupling protein 3 (mitochondrial,

Other possible sequelae of mitochondrial dysfunction include reduced redox potentials of cellular membranes, dysfunction of the mitochondrial permeability transition pore and activation of initiator and executioner caspases, each one of which may further contribute to the cell death cascade (50,51). *In vitro* studies have shown that N-terminal huntingtin fragments may directly impair mitochondrial function, resulting in calcium abnormalities and subsequent energy deficiency (52). Consistent with a link between mitochondrial derangement and the pathological phenotype of HD, there are a number of mitochondrial inhibitors that act at complexes of the electron transport chain, resulting in high-energy phosphate deficiency and reduced cellular levels of ATP, mimicking the behavioral and neuropathological phenotype of HD in both primates and rodents (53–57). Accidental ingestion of the complex II inhibitor, 3-nitropropionic acid, in humans results in a clinical and pathological phenotype observed in HD patients (58) and has been used as an experimental model of HD (53).

It has been suggested that the altered transcriptional regulation of nuclear-encoded mitochondrial genes may be involved in HD pathogenesis (33,45,59). Of great interest and of relevance to the present findings is that mHtt represses the transcription of PGC-1α (27). PGC-1α is a transcriptional co-activator regulating mitochondrial gene expression, the production of antioxidant enzymes, mitochondrial uncoupling proteins and mitochondrial ATP (25,26,60). PGC-1α mRNA is reduced in the caudate nucleus from premanifest HD patients, in transgenic HD mice and in peripheral muscle biopsies and myoblasts from manifest disease HD patients (27,28,61). Reduced levels of PGC-1α result in striatal neurodegeneration and motor abnormalities in HD mice, along with increased sensitivity to oxidative stressors, although the delivery of lentiviral-mediated PGC-1α expression into the striatum of R6/2 mice significantly improves the pathological phenotype (27). In addition, PGC-1α is greatly reduced in medium spiny neurons, those differentially effected in HD, but not in relatively spared interneurons in HD mice (27). This is consistent with our present findings showing no significant difference in COX2-positive mitochondrial density in large cholinergic neurons within the neostriatum from HD patients.

Previous studies showed that the expression of PGC-1α-dependent genes was reduced in HD caudate nucleus (61). We confirmed and extended the human HD findings of mitochondrial transcription dysregulation, showing that there were significant grade-dependent reductions of protein levels in brain lysates from HD patients, not only of PGC-1α, but also of TFAM, a mitochondrial transcription factor which functions as a DNA-packaging protein that organizes mitochondrial chromatin into the mtDNA nucleoid (42). TFAM is essential for mtDNA replication and stability through mtDNA compaction and organization of the nucleoid. TFAM knockout mice present with a significant reduction in mtDNA (62) and, as suggested, mitochondrial chromatin dynamics, along with mtDNA transcription and replication, would be markedly altered from a loss of TFAM (42). Compounds, therefore, that activate PGC-1α and TFAM may be a potential therapeutic strategy in HD.

Mitochondrial fission and fusion and their respective proteins regulate the morphology, function, integrity and topographic distribution of mitochondria, as well as trafficking of mitochondria (63). Mitochondrial morphogenesis can negatively impact important cellular mechanisms and exacerbate neuronal death. Although under normal circumstances there is equilibrium between each of these processes (35,36,64), any perturbation in mitochondrial dynamics may certainly result in mitochondrial dysfunction and mitophagy (65). As such, alterations in the proteins that control the complementary functions of fission and fusion and mitochondrial stability may trigger cell death. There is recent and emerging evidence over the past decade that mitochondrial dynamics are disrupted in neurodegenerative diseases, particularly in HD (31,33,65). Mutations or alterations in the expression of a group of conserved GTPases will disrupt the balance of mitochondrial fission and fusion. These include Drp1 and Fis1 as the principal arbiters of mitochondrial fission and fusion proteins, including the mitofusins (Mfn1 and Mfn2) that promote outer mitochondrial membrane fusion and OPA1 that facilitates inner membrane fusion and maintenance of mtDNA (37–41). Alterations in the expression pattern of mitochondrial fission/fusion proteins, shown herein as elevated levels of Drp1 and reduced levels of Mfn1 in HD caudate nucleus lysates, are consistent with altered mitochondrial dynamics, mitochondrial distribution and trafficking in HD. These observations were confirmed by histopathological analysis. Our findings suggest that an imbalance in mitochondrial fission and fusion is likely to be an important mechanism leading to mitochondrial dysfunction and subsequent neuronal loss in HD patients (31).

There is evidence from studies performed in experimental models that implicate impaired mitochondrial dynamics as a pathophysiological mechanism in HD (29,30,32,66). It has been suggested that the sequestration of trafficking proteins by mutant Htt may result in altered mitochondrial mobility (29). In addition, although the role of mutant Htt aggregates continues to be debated, it seems logical to reason that the mass effect of mutant Htt aggregates has a deleterious effect on mitochondrial dynamics. It has been reported that primary cortical neurons expressing full-length mutant Htt physically impede mitochondrial transport and that this is an early pathological event (30). Immobilized mitochondria may result in reducing energy needs throughout the neuron, especially in striatal projection neurons. It is intriguing to suggest that the improved behavioral and neuropathological phenotype in HD mouse models by the administration of select therapies that reduce Htt aggregates (4) may be the result of, at least in part, improved mitochondrial dynamics and trafficking.

There is also direct evidence that aberrant mitochondrial dynamics play a role in other human neurological disorders (67–69). A mutation in *OPA1*, an inner-membrane-localized, dynamin-related protein involved in fusion, causes autosomal dominant optic atrophy (ADOA), the most common form of

proton carrier) (*UCP3*), StAR-related lipid transfer (*START*) domain containing 3 (*STARD3*) and seven solute mitochondrial carrier family 25 genes (*SLC25A37*; *SLC25A25*, phosphate carrier; *SLC25A20*, carnitine/acylcarnitine translocase; *SLC25A2*, ornithine transporter; *SLC25A17*, peroxisomal membrane protein, 34 kDa; *SLC25A13*, citrin; and *SLC25A1*, citrate transporter member 1).

inherited optic atrophy (69). OPA1 interacts with Mfn1 in promoting fusion (70) and in remodeling mitochondrial cristae (71). There are prominent morphological alterations and defects in mitochondrial trafficking and distribution in ADOA, in addition to marked changes in the mitochondrial architecture with a tubular conformation of mitochondria, and alternating areas of fragmentation with an irregular spatial distribution (69). Muscle biopsies in ADOA show ragged-red fibers and COX2-negative fibers that are typical for mtDNA mitochondriopathies. In addition, mutations in Mfn2 result in an autosomal dominant variant of Charcot–Marie–Tooth disease, a hereditary neurological disorder presenting as a motor and sensory neuropathy (72,73). There is a significant problem in mitochondrial motility in this disorder. In Alzheimer's disease, impaired mitochondrial fission and fusion are notable features (68). Mitochondria are redistributed away from axons and limited to the soma of hippocampal pyramidal neurons. Levels of Drp1, OPA1, Mfn1 and Mfn2 are significantly reduced, in contrast to increased levels of Fis1, another mitochondrial fission protein. It has recently been reported that conditional deletion of mitofusins in mice results in mitochondrial dysfunction, increased levels of mtDNA mutations and subsequent death (74). As such, the marked reduction in Mfn2 in HD patients reported herein may contribute to the significant derangement in the mitochondrial gene expression observed in HD patients.

PCR array studies using postmortem brain samples from HD subjects have showed great numbers of gene expression changes, with the greatest number of changes and magnitude of increased expression in the caudate nucleus (75,76). Although neuronal dysfunction and loss have been identified in other regions of the brain, the earliest and most striking neuropathological changes are found in the neostriatum (3), and this, therefore, suggests that the gene alterations in the striatum have the greatest pathophysiological relevance. Studies showing preferential striatal gene changes are highly germane to the proposed pathophysiological mechanisms in HD, the goal of which is to provide insight into disease pathogenesis.

In the present findings, mitochondrial PCR array profiling was associated with alterations in genes involved with the membrane potential, mitochondrial transport and localization, inner and outer membrane translocation and apoptosis. Since there is a marked and progressive loss of neurons, with a concomitant increase in astrogliosis and microglia, in the neostriatum of HD patients, it remains to be determined whether the PCR array findings in the present study can be attributed to the neuronal findings alone. Although this has been of some concern in previous studies (75), a comparison analysis of mRNA gene levels from HD caudate tissue homogenates and laser-capture microdissected caudate neurons showed strong similarities in gene expression and the direction of gene changes (75).

The PCR array findings involve both downregulated and upregulated mRNA expression and may reflect not only the pathophysiology, but to some degree compensatory mechanisms in a failed attempt at restoring normalcy. Those few downregulated genes that had a >2-fold change included 10 genes that decreased with increasing disease severity. These were *SFN*, *AFIM2*, *NEFL*, *TIMM50*, *TOMM70A*, *TOMM34*, *HSP90AA1* and three solute mitochondrial carrier family 25 genes (*SLC25A31*, adenine nucleotide translocator; *SLC25A27*; and *SLC25A23*, phosphate carrier). Of interest to these studies was *NEFL*, a gene associated with mitochondrial localization that was reduced by 13.8-fold. Mitochondrial movement and distribution in neurons depend upon the docking of mitochondria to microtubules and neurofilaments (77). Reduced NEFL expression may restrict mitochondrial translocation to areas of the cell requiring energy, with deleterious consequences. In addition, two genes associated with outer mitochondrial membrane translocation that recognize, unfold and translocate preproteins into the mitochondria, *TOMM70A* and *TOMM34*, were also greatly decreased. Properly functioning mitochondria require the import of hundreds of proteins, most of which are synthesized in the cytoplasm and imported into mitochondria by mitochondrial translocators (78). *TOMM70A* and *TOMM34* play an important role in translocating nuclear-encoded mitochondrial proteins, including ADP/ATP carriers and the uncoupling proteins. As such, downregulation of these genes may impact energy production. Lastly, reduced expression of *SLC25A23* may result in altered small molecule transport associated with calcium binding (79).

Although there were 57 mRNA changes showing gene upregulation in the caudate nucleus from HD patients with a $\geq$2-fold increase in expression, the greatest changes ($\geq$4-fold) in upregulated mRNA expression occurred in 19 mRNAs that included *TP53*, *SOD2*, *SFN*, *BCL2L1*, *BAK1*, *TIMM44*, *TAZ*, *FXC1*, *TOMM40*, *UPC3*, *STARD3* and three solute mitochondrial carrier family 25 genes (*SLC25A37*, *SLC25A2* and *SLC25A13*) (Table 1).

TP53 responds to cell stress by regulating genes that influence cell cycle phenomena, including cell arrest, apoptosis, senescence, DNA repair and changes in metabolism (80). P53 is increased in brains from HD patients and, as such, it has been suggested that the mutant huntingtin protein interacts with p53, altering transcriptional and subsequent cell cycling events (81,82). A deletion of p53 reduces mitochondrial membrane depolarization and cell death in HD (82). SOD2, an antioxidant mitochondrial matrix protein-binding manganese, is critically vital in reducing superoxide molecules and oxidative stress, a pathophysiological mechanism associated with HD (83). Upregulation of SOD2 is neuroprotective in the 3-nitropropionic acid toxin model of HD (84) and in the present findings may be an attempt to respond to reactive oxygen species and to promote neuronal survival. In addition, *SFN (14-3-3)* helps to determine DNA damage and modulates functional cellular pathways of cell arrest or death (85). Although the suppression of *14-3-3 zeta* blocks the formation of huntingtin inclusion bodies (86), *SFN*'s upregulation may be a compensatory mechanism, acting to facilitate the incorporation of misfolded huntingtin protein into aggregates in overwhelmed neurons (86). Of interest, herein, is the finding that SFN expression is upregulated in mid-disease and downregulated at end-stage disease, consistent with an early effort at cellular rescue. The *BCL2L1* gene belongs to the BCL-2 protein family and can act as an anti- or pro-apoptotic regulator. *BCL2L1* may also regulate channel opening of the outer mitochondrial membrane, controlling the release of ROS and cytochrome *c*. Cytochrome c is significantly increased in the cytosol of neurons in HD and induces the apoptotic cascade (51). As such, altered *BCL2L1* upregulation may contribute

to the further demise of neurons. *BAK1*, another *BCL2* protein family gene, also functions to induce apoptosis. Both of the latter two genes have their greatest upregulation in Grade 2 samples with less expression in severe and very severe HD striatal tissue samples, suggesting that apoptosis may be an early pathophysiological event. Two genes linked with the inner mitochondrial membrane (*TIMM44* and *TAZ*) catalyze general acyl exchange between phospholipids (87) and, as such, any perturbation in either gene may disrupt mitochondrial lipid distribution, resulting in mitochondrial dysfunction. *TOMM40* upregulation was increased ~35-fold. The *TOMM40* machinery is essential for protein import into the mitochondrion and in promoting mitochondrial respiration (88). ATP is required for the formation of the *TOMM40* complex (89) and, therefore, the inordinate upregulation of *TOMM40* expression may be a failed compensatory process, resulting from the early bioenergetic deficit of reduced ATP in HD. Mitochondrial uncoupling proteins (UCPs) facilitate reciprocal ion transfer from the inner and outer mitochondrial membrane for the production of ATP. UCPs are also suggested to protect mitochondria from lipid-induced oxidative stress (90). *UCP3* expression is upregulated ~38-fold in the caudate nucleus in the present study, and may be involved in a response aimed at reducing mitochondrial lipid peroxidation. *STARD3*, a member of a subfamily of lipid-trafficking proteins involved in exporting cholesterol, is upregulated early at high expression levels (~18-fold). Cholesterol that is not moved into the mitochondria collects into cytoplasmic droplets, resulting in potential cytotoxicity (91).

The present studies used a diverse methodological approach in examining mitochondrial dysfunction and altered mitochondrial dynamics in HD patients that include morphological, biochemical and PCR array procedures. These techniques provide parallel and complementary data that are consistent with mitochondrial dysfunction in HD patients. To that end, our findings present the strongest evidence to date that mitochondrial impairment and loss play a critical role in neuronal loss and disease progression in HD patients and, as such, have further implications for therapeutic strategies to reduce bioenergetic defects.

MATERIALS AND METHODS

Brain tissue specimens

Postmortem neostriatal tissue specimens from 35 adult-onset HD patients (9 Grade 2 patients, 10 Grade 3 patients and 16 Grade 4 patients; mean age 64.3 years; range 56–71 years) and 14 age-matched control patients without any known neurologic disease (mean age 66.2 years; range 61–71 years). The sources of the brain tissue specimens were from the Bedford Veterans Affairs Medical Center Brain Tissue Archive, the New York Brain Bank at Columbia University and the Boston University Brain Bank Tissue Archive. Collection and archiving of tissue samples were treated in a similar manner. Drs Ferrante, McKee and Vonsattel have been collaborators for over 20 years and have co-authored manuscripts in preparing human brains for research (92,93). The postmortem intervals did not exceed 18 h (HD patients' mean time 8.6 h, range 5–17 h; control patients mean time 10.2 h, range 3–18 h). Each HD patient had been clinically diagnosed based on a family history of HD and symptoms of HD. The diagnosis of HD was confirmed by neuropathological examination and graded by severity (91). Neostriatal tissue blocks 0.5 cm in thickness were dissected fresh, fixed by placement in ice-cold (4°C) 2% paraformaldehyde-lysine and 0.2% periodate for 24–36 h, rinsed in 0.1 M sodium phosphate, pH 7.4, and placed in ice-cold cryoprotectant (4°C) in increasing concentrations of 10 and 20% glycerol and 2% DMSO over a 36 h period. Frozen 50 mm serial sections of the neostriatal tissue blocks were cut in the coronal plane and stored in saline buffer containing 0.08% sodium azide at 4°C for immunocytochemistry and immunofluorescence. Contiguous dissected fresh tissue blocks were rapidly quenched and stored at −80°C for western analysis and RT2-PCR array.

Immunocytochemistry

Immunohistochemical localization of antibodies to calbindin (SWANT, diluted 1:1000) identifying medium-sized spiny striatal neurons in HD (2), and mitochondria markers using Mt-COX2 (Abcam, diluted 1:500), SOD2 (Abcam, diluted 1:500), cytochrome *c* (Zymed, diluted 1:500) (51), and markers of both mitochondrial fission (Abcam, DNM1L (DRP1), diluted 1:500) and fusion (Santa Cruz Biotechnology, USA, Mfn1, diluted 1:200), was performed with conjugated second antibodies. All dilutions of primary antiserum contained 0.08% Triton X-100, 2% normal goat serum. Tissue sections were preincubated in absolute methanol–0.3% hydrogen peroxide for 30 min, washed for three 10 min periods in PBS (pH 7.4), incubated in 10% normal goat serum (GIBCO) for 1 h, incubated free-floating in primary antiserum at room temperature for 12–18 h, washed as above, placed in peroxidase-conjugated goat anti-rabbit IgG (Chemicon, diluted 1:1000 in PBS), washed as above and incubated with 3,3′-diaminobenzidine-HCl (1 mg/ml) in 1 M Tris–HCl (pH 7.0) containing 0.005% hydrogen peroxide. To test for the specificity of the antisera used in this study, we performed preabsorption with excess target proteins and omission of primary and secondary antibodies to determine the amount of background generated from the detection assay.

Immunofluorescent staining

Immunofluorescent staining was performed in all HD and age-matched control caudate nucleus tissue specimens by first incubating striatal tissue sections in the calbindin polyclonal antiserum (diluted 1:600) and in separate subsequent incubations using the mitochondrial markers Mt-COX2, SOD2 and cytochrome *c*. Antisera dilutions were made up in 1 M Tris–HCl (pH 7) buffer containing 0.3% Triton X-100 for 24–72 h at 4°C. Sections were then rinsed in PBS (three 10 min washes). For immunofluorescent visualization, sections were incubated in donkey anti-rabbit Cy3-conjugated (Jackson ImmunoResearch Laboratory, dilution 1:200) antibodies to detect Mt-COX2 and cytochrome *c*, or donkey anti-mouse Cy3-conjugated (Jackson ImmunoResearch Laboratory, dilution 1:200) antibodies for SOD2. Horse anti-rabbit FITC-conjugated (Vector, dilution 1:200) or horse anti-mouse FITC-conjugated (Vector, dilution 1:200) antibodies were used to detect calbindin antibodies and were counterstained with DAPI. Sections were incubated in the dark with FITC

conjugate for 2 h at 20°C, rinsed three times in PBS and incubated with Cy3 for 2 h at 20°C. Deletion of the calbindin antisera resulted in no green fluorescence, whereas deletion of the Mt-COX2, SOD2 and cytochrome *c* antisera resulted in no red fluorescence. Sections were wet-mounted and cover-slipped in Vectashield mounting medium (Vector) and analyzed using fluorescence microscopy.

Microscopy and image analysis

Light and fluorescence microscopy were performed using a Nikon Eclipse E800 microscope with a Spot RT digital camera. Combined immunostaining was incomplete in some of the postmortem HD and control specimens. As such, digital imaging analysis was performed on 8 Grade 2 patients, 7 Grade 3 patients, 12 Grade 4 patients and 10 age-matched control patients. Images were captured at 0.25 μm intervals. Stacked images were deconvoluted with a constrained iterative algorithm, using a cooled charge-coupled device camera (Retiga-2000R: Q-Imaging). Optical sections were captured using NIS-Elements AR (Nikon Instruments, Inc., Melville, NY, USA) and processed using a 3D deconvolution module. The spatial distribution of Mt-COX2- and SOD2-positive mitochondrial figures in calbindin-positive striatal neurons was determined using confocal microscopy and an image analysis program (Auto Quant 3D, MediaCybernetics, Inc., Bethesda, MD, USA). We analyzed a series of 20–25 confocal layers representing fluorescence data from striatal neurons and subsequently developed an abstract image that provided the results.

Quantification/stereology

Striatal calbindin-positive neurons (green fluorescent cells) were chosen randomly by the image analysis system, as not to bias the results, and absolute perikaryal mitochondrial counts for the Mt-COX2 and SOD2 markers were quantitated. A computer-automated threshold/segmentation method was used for separating clustered objects, identifying their volume, and density/number of objects in 3D confocal microscopy. Cellular volumes were computed from the stacked images, and the density of mitochondria was determined in age-matched control, Grade 2 HD and Grade 4 tissue samples. Absolute counts of Mt-COX2- and SOD2-positive mitochondrial figures within the calbindin-positive striatal neurons from the medial caudate nucleus were performed with the experimenter blinded to disease conditions. Counts were performed with each mitochondrial figure identified independently by two investigators (J.P.M., J.K.) using Image-Pro Plus (MediaCybernetics, Inc., Bethesda, MD, USA). There were no significant intra-rater differences. The accuracy of the counts was further examined and verified by R.J.F. Over 100 neurons from each group of HD and control specimens were used for mitochondrial quantitation.

Western blot

Western blot analyses in neostriatal tissue specimens were performed on all 35 Grade 2, 3 and 4 HD patients and 16 age-matched control subjects. Brain lysates from the medial caudate nucleus were obtained by fractionating tissue samples in 100 mM Tris (pH 7.4) buffer containing 1% Triton X-100, 150 mM NaCl, 1 mM sodium orthovanadate, 5 mM sodium fluoride, 3 mM PMSF, 3 mM DTT, 0.5 μg/ml leupeptin and 10 μg/ml aprotinin. Thirty micrograms of protein from tissue lysates from the medial caudate nucleus was electrophoresed under reducing conditions on 8% polyacrylamide gels. Proteins were transferred to a nitrocellulose membrane (Bio-Rad, Hercules, CA, USA). Nonspecific binding was inhibited by incubation in Tris-buffered saline (TBST; 50 mM Tris–HCl, pH 8.0, 0.9% NaCl and 0.1% Tween 20) containing 5% nonfat dried milk for 0.5 h. Primary antibodies against PGC-1α (1:1000, Abcam, USA), mitochondrial transcription factor A (TFAM) (1:1000, Abcam), DNM1L (DRP1 1:1000, Abcam), MfN1 (1:1000, Santa Cruz Biotechnology) were diluted in TBST with 1% milk and exposed to membranes overnight at 4°C. Membranes were washed and incubated for 2 h with HRP-conjugated secondary antibodies. Immunoreactive proteins were detected according to the enhanced chemiluminescence protocol (Pierce Biotechnology, Rockford, IL, USA). Results were standardized to alpha tubulin and analyzed using NIH Image.

PCR array

Total RNA from Grade 2, 3 and 4 HD patients and age-matched control subjects within eight specimens from each group representing the lowest postmortem hours from the medial caudate nucleus were extracted using a Trizol® reagent (Invitrogen, Frederick, MD, USA). Total RNAs were treated with RNase-free DNase and isolated using an RT^2 qPCR-Grade RNA Isolation Kit (SABioscience, Frederick, MD, USA). RT reaction was performed with 400 ng of total RNA using an RT^2 First-strand Kit (SABioscience). The quality of RNA was confirmed by using an RT^2 RNA QC PCR Array Kit (SABioscience). Two hundred nanograms of random-primed cDNAs were processed for quantitative real-time reverse-transcriptase PCR (RT-qPCR) of 84 genes involved in biogenesis and function of mitochondria and 12 housekeeping genes including internal controls by using an RT^2 Profiler^{TM} PCR Array Kit (RT^2 ProfilerTM PCR Array Human Mitochondria, PAHS-087A, SABioscience) and an ABI 7300 real-time PCR system (Applied Biosystems, Foster City, CA, USA). PCR products were quantified by measuring SYBR Green fluorescent dye incorporation with ROX dye reference. Four independent pair-wise comparisons were performed to evaluate scored differences in gene changes with a correlation coefficient of $R > 0.990$. An integrated web-based software package for the PCR Array System performed $\Delta\Delta C_t$-based fold-change calculations from the uploaded raw threshold cycle data.

Statistics

Interval scale data involving more than two groups were analyzed using two-way analysis of variance. If an overall significant difference was detected, multiple comparisons were performed with Fisher's least significant difference test.

ACKNOWLEDGEMENTS

Brain tissue specimens were generously donated by Dr Jean Paul Vonsattel from the New York Brain Bank of Columbia University (PO1-AG07232, R37-AG15437, P50-AG08702, Hereditary Disease Foundation, Iseman Fund, Louis and Rachel Rudin Foundation) and Dr Ann McKee from the Boston University Alzheimer's Disease Brain Bank (NIA P30AG13846).

Conflict of Interest statement. None declared.

FUNDING

This work was supported by the Jerry McDonald Research Fund in Huntington's Disease at the Boston University School of Medicine, National Institutes of Health Grants NS045806 (R.J.F.) and NS058793 (R.J.F.), and the Veterans Administration VISN 1.

REFERENCES

1. Ferrante, R.J., Beal, M.F., Kowall, N.W., Richardson, E.P. Jr and Martin, J.B. (1987) Sparing of acetylcholinesterase-containing striatal neurons in Huntington's disease. *Brain Res.*, **411**, 162–166.
2. Ferrante, R.J., Kowall, N.W. and Richardson, E.P. Jr (1991) Proliferative and degenerative changes in striatal spiny neurons in Huntington's disease: a combined study using the section-Golgi method and calbindin D28k immunocytochemistry. *J. Neurosci.*, **11**, 3877–3887.
3. Hersch, S.M., Rosas, H.R. and Ferrante, R.J. (2004) Neuropathology and pathophysiology of Huntington's disease. In Watts, R.L. and Koller, W.C. (eds), *Movement Disorders: Neurologic Principles and Practice*, McGraw-Hill, New York, NY, pp. 503–523.
4. Stack, E.C. and Ferrante, R.J. (2007) Huntington's disease: progress and potential in the field. *Expert Opin. Investig. Drugs*, **16**, 1933–1953.
5. Benard, G., Bellance, N., James, D., Parrone, P., Fernandez, H., Letellier, T. and Rossignol, R. (2007) Mitochondrial bioenergetics and structural network organization. *J. Cell Sci.*, **120**, 838–848.
6. Kann, O. and Kovacs, R. (2007) Mitochondria and neuronal activity. *Am. J. Physiol. Cell Physiol.*, **292**, C641–C657.
7. Browne, S.E. and Beal, M.F. (2004) The energetics of Huntington's disease. *Neurochem. Res.*, **29**, 531–546.
8. Browne, S.E. (2008) Mitochondria and Huntington's disease pathogenesis: insight from genetic and chemical models. *Ann. N Y Acad. Sci.*, **1147**, 358–382.
9. Reddy, P.H., Mao, P. and Manczak, M. (2009) Mitochondrial structural and functional dynamics in Huntington's disease. *Brain Res. Rev.*, **61**, 33–48.
10. Damiano, M., Galvan, L., Deglon, N. and Brouillet, E. (2010) Mitochondria in Huntington's disease. *Biochim. Biophys. Acta*, **1802**, 52–61.
11. Tellez-Nagel, I., Johnson, A.B. and Terry, R.D. (1974) Studies on brain biopsies of patients with Huntington's chorea. *J. Neuropathol. Exp. Neurol.*, **33**, 308–332.
12. Howell, N., Bindoff, L.A., McCullough, D.A., Kubacka, I., Poulton, J., Mackey, D., Taylor, L. and Turnbull, D.M. (1991) Leber hereditary optic neuropathy: identification of the same mitochondrial ND1 mutation in six pedigrees. *Am. J. Hum. Genet.*, **49**, 939–950.
13. Jun, A.S., Brown, M.D. and Wallace, D.C. (1994) A mitochondrial DNA mutation at nucleotide pair 14459 of the NADH dehydrogenase subunit 6 gene associated with maternally inherited Leber hereditary optic neuropathy and dystonia. *Proc. Natl Acad. Sci. USA*, **91**, 6206–6210.
14. Brennan, W.A. Jr, Bird, E.D. and Aprille, J.R. (1985) Regional mitochondrial respiratory activity in Huntington's disease brain. *J. Neurochem.*, **44**, 1948–1950.
15. Mann, V.M., Cooper, J.M., Javoy-Agid, F., Agid, Y., Jenner, P. and Schapira, A.H. (1990) Mitochondrial function and parental sex effect in Huntington's disease. *Lancet*, **336**, 749.
16. Parker, W.D. Jr, Boyson, S.J., Luder, A.S. and Parks, J.K. (1990) Evidence for a defect in NADH: ubiquinone oxidoreductase (complex I) in Huntington's disease. *Neurology*, **40**, 1231–1234.
17. Gu, M., Gash, M.T., Mann, V.M., Javoy-Agid, F., Cooper, J.M. and Schapira, A.H. (1996) Mitochondrial defect in Huntington's disease caudate nucleus. *Ann. Neurol.*, **39**, 385–389.
18. Browne, S.E., Bowling, A.C., MacGarvey, U., Baik, M.J., Berger, S.C., Muqit, M.M., Bird, E.D. and Beal, M.F. (1997) Oxidative damage and metabolic dysfunction in Huntington's disease: selective vulnerability of the basal ganglia. *Ann. Neurol.*, **41**, 646–653.
19. Tabrizi, S.J., Cleeter, M.W., Xuereb, J., Taanman, J.W., Cooper, J.M. and Schapira, A.H. (1999) Biochemical abnormalities and excitotoxicity in Huntington's disease brain. *Ann. Neurol.*, **45**, 25–32.
20. Fukui, H. and Moraes, C.T. (2007) Extended polyglutamine repeats trigger a feedback loop involving the mitochondrial complex III, the proteasome and huntingtin aggregates. *Hum. Mol. Genet.*, **16**, 783–797.
21. Guidetti, P., Charles, V., Chen, E.Y., Reddy, P.H., Kordower, J.H., Whetsell, W.O. Jr, Schwarcz, R. and Tagle, D.A. (2001) Early degenerative changes in transgenic mice expressing mutant huntingtin involve dendritic abnormalities but no impairment of mitochondrial energy production. *Exp. Neurol.*, **169**, 340–350.
22. Mastrogiacomo, F., LaMarche, J., Dozic, S., Lindsay, G., Bettendorff, L., Robitaille, Y., Schut, L. and Kish, S.J. (1996) Immunoreactive levels of alpha-ketoglutarate dehydrogenase subunits in Friedreich's ataxia and spinocerebellar ataxia type 1. *Neurodegeneration*, **5**, 27–33.
23. Matsuishi, T., Sakai, T., Naito, E., Nagamitsu, S., Kuroda, Y., Iwashita, H. and Kato, H. (1996) Elevated cerebrospinal fluid lactate/pyruvate ratio in Machado–Joseph disease. *Acta Neurol. Scand.*, **93**, 72–75.
24. Dunah, A.W., Jeong, H., Griffin, A., Kim, Y.M., Standaert, D.G., Hersch, S.M., Mouradian, M.M., Young, A.B., Tanese, N. and Krainc, D. (2002) Sp1 and TAFII130 transcriptional activity disrupted in early Huntington's disease. *Science*, **296**, 2238–2243.
25. Lin, J., Wu, P.H., Tarr, P.T., Lindenberg, K.S., St-Pierre, J., Zhang, C.Y., Mootha, V.K., Jager, S., Vianna, C.R., Reznick, R.M. *et al.* (2004) Defects in adaptive energy metabolism with CNS-linked hyperactivity in PGC-1alpha null mice. *Cell*, **119**, 121–135.
26. Lin, J., Yang, R., Tarr, P.T., Wu, P.H., Handschin, C., Li, S., Yang, W., Pei, L., Uldry, M., Tontonoz, P. *et al.* (2005) Hyperlipidemic effects of dietary saturated fats mediated through PGC-1beta coactivation of SREBP. *Cell*, **120**, 261–273.
27. Cui, L., Jeong, H., Borovecki, F., Parkhurst, C.N., Tanese, N. and Krainc, D. (2006) Transcriptional repression of PGC-1alpha by mutant huntingtin leads to mitochondrial dysfunction and neurodegeneration. *Cell*, **127**, 59–69.
28. Chaturvedi, R.K., Adhihetty, P., Shukla, S., Hennessy, T., Calingasan, N., Yang, L., Starkov, A., Kiaei, M., Cannella, M., Sassone, J. *et al.* (2009) Impaired PGC-1alpha function in muscle in Huntington's disease. *Hum. Mol. Genet.*, **18**, 3048–3065.
29. Trushina, E., Dyer, R.B., Badger, J.D. II, Ure, D., Eide, L., Tran, D.D., Vrieze, B.T., Legendre-Guillemin, V., McPherson, P.S., Mandavilli, B.S. *et al.* (2004) Mutant huntingtin impairs axonal trafficking in mammalian neurons *in vivo* and *in vitro*. *Mol. Cell. Biol.*, **24**, 8195–8209.
30. Chang, D.T., Rintoul, G.L., Pandipati, S. and Reynolds, I.J. (2006) Mutant huntingtin aggregates impair mitochondrial movement and trafficking in cortical neurons. *Neurobiol. Dis.*, **22**, 388–400.
31. Knott, A.B. and Bossy-Wetzel, E. (2008) Impairing the mitochondrial fission and fusion balance: a new mechanism of neurodegeneration. *Ann. N Y Acad. Sci.*, **1147**, 283–292.
32. Wang, H., Lim, P.J., Karbowski, M. and Monteiro, M.J. (2009) Effects of overexpression of huntingtin proteins on mitochondrial integrity. *Hum. Mol. Genet.*, **18**, 737–752.
33. Su, B., Wang, X., Zheng, L., Perry, G., Smith, M.A. and Zhu, X. (2010) Abnormal mitochondrial dynamics and neurodegenerative diseases. *Biochim. Biophys. Acta*, **1802**, 135–142.
34. Bereiter-Hahn, J., Voth, M., Mai, S. and Jendrach, M. (2008) Structural implications of mitochondrial dynamics. *Biotechnol. J.*, **3**, 765–780.
35. Shaw, J.M. and Nunnari, J. (2002) Mitochondrial dynamics and division in budding yeast. *Trends Cell Biol.*, **12**, 178–184.
36. Scott, S.V., Cassidy-Stone, A., Meeusen, S.L. and Nunnari, J. (2003) Staying in aerobic shape: how the structural integrity of mitochondria and mitochondrial DNA is maintained. *Curr. Opin. Cell Biol.*, **15**, 482–488.
37. Otsuga, D., Keegan, B.R., Brisch, E., Thatcher, J.W., Hermann, G.J., Bleazard, W. and Shaw, J.M. (1998) The dynamin-related GTPase,

Dnm1p, controls mitochondrial morphology in yeast. *J. Cell Biol.*, **143**, 333–349.
38. Bleazard, W., McCaffery, J.M., King, E.J., Bale, S., Mozdy, A., Tieu, Q., Nunnari, J. and Shaw, J.M. (1999) The dynamin-related GTPase Dnm1 regulates mitochondrial fission in yeast. *Nat. Cell Biol.*, **1**, 298–304.
39. Dimmer, K.S. and Scorrano, L. (2006) (De)constructing mitochondria: what for? *Physiology (Bethesda)*, **21**, 233–241.
40. Mozdy, A.D., McCaffery, J.M. and Shaw, J.M. (2000) Dnm1p GTPase-mediated mitochondrial fission is a multi-step process requiring the novel integral membrane component Fis1p. *J. Cell Biol.*, **151**, 367–380.
41. Jakobs, S., Martini, N., Schauss, A.C., Egner, A., Westermann, B. and Hell, S.W. (2003) Spatial and temporal dynamics of budding yeast mitochondria lacking the division component Fis1p. *J. Cell Sci.*, **116**, 2005–2014.
42. Kaufman, B.A., Durisic, N., Mativetsky, J.M., Costantino, S., Hancock, M.A., Grutter, P. and Shoubridge, E.A. (2007) The mitochondrial transcription factor TFAM coordinates the assembly of multiple DNA molecules into nucleoid-like structures. *Mol. Biol. Cell*, **18**, 3225–3236.
43. Lee, H.C. and Wei, Y.H. (2000) Mitochondrial role in life and death of the cell. *J. Biomed. Sci.*, **7**, 2–15.
44. Beal, M.F. (2005) Mitochondria take center stage in aging and neurodegeneration. *Ann. Neurol.*, **58**, 495–505.
45. Bossy-Wetzel, E., Petrilli, A. and Knott, A.B. (2008) Mutant huntingtin and mitochondrial dysfunction. *Trends Neurosci.*, **31**, 609–616.
46. Tabrizi, S.J., Workman, J., Hart, P.E., Mangiarini, L., Mahal, A., Bates, G., Cooper, J.M. and Schapira, A.H. (2000) Mitochondrial dysfunction and free radical damage in the Huntington R6/2 transgenic mouse. *Ann. Neurol.*, **47**, 80–86.
47. Smith, K.M., Matson, S., Matson, W.R., Cormier, K., Del Signore, S.J., Hagerty, S.W., Stack, E.C., Ryu, H. and Ferrante, R.J. (2006) Dose ranging and efficacy study of high-dose coenzyme Q10 formulations in Huntington's disease mice. *Biochim. Biophys. Acta*, **1762**, 616–626.
48. Acevedo-Torres, K., Berrios, L., Rosario, N., Dufault, V., Skatchkov, S., Eaton, M.J., Torres-Ramos, C.A. and Ayala-Torres, S. (2009) Mitochondrial DNA damage is a hallmark of chemically induced and the R6/2 transgenic model of Huntington's disease. *DNA Repair (Amst.)*, **8**, 126–136.
49. Oliveira, J.M., Jekabsons, M.B., Chen, S., Lin, A., Rego, A.C., Goncalves, J., Ellerby, L.M. and Nicholls, D.G. (2007) Mitochondrial dysfunction in Huntington's disease: the bioenergetics of isolated and *in situ* mitochondria from transgenic mice. *J. Neurochem.*, **101**, 241–249.
50. Green, D.R. and Reed, J.C. (1998) Mitochondria and apoptosis. *Science*, **281**, 1309–1312.
51. Kiechle, T., Dedeoglu, A., Kubilus, J., Kowall, N.W., Beal, M.F., Friedlander, R.M., Hersch, S.M. and Ferrante, R.J. (2002) Cytochrome C and caspase-9 expression in Huntington's disease. *Neuromolecular Med.*, **1**, 183–195.
52. Panov, A.V., Gutekunst, C.A., Leavitt, B.R., Hayden, M.R., Burke, J.R., Strittmatter, W.J. and Greenamyre, J.T. (2002) Early mitochondrial calcium defects in Huntington's disease are a direct effect of polyglutamines. *Nat. Neurosci.*, **5**, 731–736.
53. Beal, M.F., Brouillet, E., Jenkins, B.G., Ferrante, R.J., Kowall, N.W., Miller, J.M., Storey, E., Srivastava, R., Rosen, B.R. and Hyman, B.T. (1993) Neurochemical and histologic characterization of striatal excitotoxic lesions produced by the mitochondrial toxin 3-nitropropionic acid. *J. Neurosci.*, **13**, 4181–4192.
54. Brouillet, E., Hantraye, P., Ferrante, R.J., Dolan, R., Leroy-Willig, A., Kowall, N.W. and Beal, M.F. (1995) Chronic mitochondrial energy impairment produces selective striatal degeneration and abnormal choreiform movements in primates. *Proc. Natl Acad. Sci. USA*, **92**, 7105–7109.
55. Brouillet, E., Jenkins, B.G., Hyman, B.T., Ferrante, R.J., Kowall, N.W., Srivastava, R., Roy, D.S., Rosen, B.R. and Beal, M.F. (1993) Age-dependent vulnerability of the striatum to the mitochondrial toxin 3-nitropropionic acid. *J. Neurochem.*, **60**, 356–359.
56. Palfi, S., Ferrante, R.J., Brouillet, E., Beal, M.F., Dolan, R., Guyot, M.C., Peschanski, M. and Hantraye, P. (1996) Chronic 3-nitropropionic acid treatment in baboons replicates the cognitive and motor deficits of Huntington's disease. *J. Neurosci.*, **16**, 3019–3025.
57. Schulz, J.B., Henshaw, D.R., Siwek, D., Jenkins, B.G., Ferrante, R.J., Cipolloni, P.B., Kowall, N.W., Rosen, B.R. and Beal, M.F. (1995) Involvement of free radicals in excitotoxicity *in vivo*. *J. Neurochem.*, **64**, 2239–2247.
58. Ludolph, A.C., He, F., Spencer, P.S., Hammerstad, J. and Sabri, M. (1991) 3-Nitropropionic acid-exogenous animal neurotoxin and possible human striatal toxin. *Can. J. Neurol. Sci.*, **18**, 492–498.
59. Reddy, P.H. (2008) Mitochondrial medicine for aging and neurodegenerative diseases. *Neuromolecular Med.*, **10**, 291–315.
60. Rohas, L.M., St-Pierre, J., Uldry, M., Jager, S., Handschin, C. and Spiegelman, B.M. (2007) A fundamental system of cellular energy homeostasis regulated by PGC-1alpha. *Proc. Natl Acad. Sci. USA*, **104**, 7933–7938.
61. Weydt, P., Pineda, V.V., Torrence, A.E., Libby, R.T., Satterfield, T.F., Lazarowski, E.R., Gilbert, M.L., Morton, G.J., Bammler, T.K., Strand, A.D. *et al.* (2006) Thermoregulatory and metabolic defects in Huntington's disease transgenic mice implicate PGC-1alpha in Huntington's disease neurodegeneration. *Cell Metab.*, **4**, 349–362.
62. Larsson, N.G., Wang, J., Wilhelmsson, H., Oldfors, A., Rustin, P., Lewandoski, M., Barsh, G.S. and Clayton, D.A. (1998) Mitochondrial transcription factor A is necessary for mtDNA maintenance and embryogenesis in mice. *Nat. Genet.*, **18**, 231–236.
63. Chan, D.C. (2006) Mitochondria: dynamic organelles in disease, aging, and development. *Cell*, **125**, 1241–1252.
64. Nunnari, J., Marshall, W.F., Straight, A., Murray, A., Sedat, J.W. and Walter, P. (1997) Mitochondrial transmission during mating in *Saccharomyces cerevisiae* is determined by mitochondrial fusion and fission and the intramitochondrial segregation of mitochondrial DNA. *Mol. Biol. Cell*, **8**, 1233–1242.
65. Chen, H. and Chan, D.C. (2009) Mitochondrial dynamics—fusion, fission, movement, and mitophagy—in neurodegenerative diseases. *Hum. Mol. Genet.*, **18**, R169–R176.
66. Trushina, E., Heldebrant, M.P., Perez-Terzic, C.M., Bortolon, R., Kovtun, I.V., Badger, J.D. II, Terzic, A., Estevez, A., Windebank, A.J., Dyer, R.B. *et al.* (2003) Microtubule destabilization and nuclear entry are sequential steps leading to toxicity in Huntington's disease. *Proc. Natl Acad. Sci. USA*, **100**, 12171–12176.
67. DiMauro, S. and Schon, E.A. (2008) Mitochondrial disorders in the nervous system. *Annu. Rev. Neurosci.*, **31**, 91–123.
68. Wang, X., Su, B., Lee, H.G., Li, X., Perry, G., Smith, M.A. and Zhu, X. (2009) Impaired balance of mitochondrial fission and fusion in Alzheimer's disease. *J. Neurosci.*, **29**, 9090–9103.
69. Spinazzi, M., Cazzola, S., Bortolozzi, M., Baracca, A., Loro, E., Casarin, A., Solaini, G., Sgarbi, G., Casalena, G., Cenacchi, G. *et al.* (2008) A novel deletion in the GTPase domain of OPA1 causes defects in mitochondrial morphology and distribution, but not in function. *Hum. Mol. Genet.*, **17**, 3291–3302.
70. Cipolat, S., Martins de Brito, O., Dal Zilio, B. and Scorrano, L. (2004) OPA1 requires mitofusin 1 to promote mitochondrial fusion. *Proc. Natl Acad. Sci. USA*, **101**, 15927–15932.
71. Cipolat, S., Rudka, T., Hartmann, D., Costa, V., Serneels, L., Craessaerts, K., Metzger, K., Frezza, C., Annaert, W., D'Adamio, L. *et al.* (2006) Mitochondrial rhomboid PARL regulates cytochrome *c* release during apoptosis via OPA1-dependent cristae remodeling. *Cell*, **126**, 163–175.
72. Lawson, V.H., Graham, B.V. and Flanigan, K.M. (2005) Clinical and electrophysiologic features of CMT2A with mutations in the mitofusin 2 gene. *Neurology*, **65**, 197–204.
73. Zuchner, S., Mersiyanova, I.V., Muglia, M., Bissar-Tadmouri, N., Rochelle, J., Dadali, E.L., Zappia, M., Nelis, E., Patitucci, A., Senderek, J. *et al.* (2004) Mutations in the mitochondrial GTPase mitofusin 2 cause Charcot–Marie–Tooth neuropathy type 2A. *Nat. Genet.*, **36**, 449–451.
74. Chen, H., Vermulst, M., Wang, Y.E., Chomyn, A., Prolla, T.A., McCaffery, J.M. and Chan, D.C. (2010) Mitochondrial fusion is required for mtDNA stability in skeletal muscle and tolerance of mtDNA mutations. *Cell*, **141**, 280–289.
75. Hodges, A., Strand, A.D., Aragaki, A.K., Kuhn, A., Sengstag, T., Hughes, G., Elliston, L.A., Hartog, C., Goldstein, D.R., Thu, D. *et al.* (2006) Regional and cellular gene expression changes in human Huntington's disease brain. *Hum. Mol. Genet.*, **15**, 965–977.
76. Thomas, E.A. (2006) Striatal specificity of gene expression dysregulation in Huntington's disease. *J. Neurosci. Res.*, **84**, 1151–1164.
77. Wagner, O.I., Lifshitz, J., Janmey, P.A., Linden, M., McIntosh, T.K. and Leterrier, J.F. (2003) Mechanisms of mitochondria-neurofilament interactions. *J. Neurosci.*, **23**, 9046–9058.

78. Edmonson, A.M., Mayfield, D.K., Vervoort, V., DuPont, B.R. and Argyropoulos, G. (2002) Characterization of a human import component of the mitochondrial outer membrane, TOMM70A. *Cell Commun. Adhes.*, **9**, 15–27.
79. Bassi, M.T., Manzoni, M., Bresciani, R., Pizzo, M.T., Della Monica, A., Barlati, S., Monti, E. and Borsani, G. (2005) Cellular expression and alternative splicing of SLC25A23, a member of the mitochondrial Ca2+-dependent solute carrier gene family. *Gene*, **345**, 173–182.
80. Vogelstein, B., Lane, D. and Levine, A.J. (2000) Surfing the p53 network. *Nature*, **408**, 307–310.
81. Steffan, J.S., Kazantsev, A., Spasic-Boskovic, O., Greenwald, M., Zhu, Y.Z., Gohler, H., Wanker, E.E., Bates, G.P., Housman, D.E. and Thompson, L.M. (2000) The Huntington's disease protein interacts with p53 and CREB-binding protein and represses transcription. *Proc. Natl Acad. Sci. USA*, **97**, 6763–6768.
82. Bae, B.I., Xu, H., Igarashi, S., Fujimuro, M., Agrawal, N., Taya, Y., Hayward, S.D., Moran, T.H., Montell, C., Ross, C.A. *et al.* (2005) p53 mediates cellular dysfunction and behavioral abnormalities in Huntington's disease. *Neuron*, **47**, 29–41.
83. Browne, S.E., Ferrante, R.J. and Beal, M.F. (1999) Oxidative stress in Huntington's disease. *Brain Pathol.*, **9**, 147–163.
84. Madhavan, L., Ourednik, V. and Ourednik, J. (2008) Neural stem/progenitor cells initiate the formation of cellular networks that provide neuroprotection by growth factor-modulated antioxidant expression. *Stem Cells*, **26**, 254–265.
85. Dougherty, M.K. and Morrison, D.K. (2004) Unlocking the code of 14-3-3. *J. Cell Sci.*, **117**, 1875–1884.
86. Omi, K., Hachiya, N.S., Tanaka, M., Tokunaga, K. and Kaneko, K. (2008) 14-3-3zeta is indispensable for aggregate formation of polyglutamine-expanded huntingtin protein. *Neurosci. Lett.*, **431**, 45–50.
87. Malhotra, A., Xu, Y., Ren, M. and Schlame, M. (2009) Formation of molecular species of mitochondrial cardiolipin. 1. A novel transacylation mechanism to shuttle fatty acids between sn-1 and sn-2 positions of multiple phospholipid species. *Biochim. Biophys. Acta*, **1791**, 314–320.
88. Humphries, A.D., Streimann, I.C., Stojanovski, D., Johnston, A.J., Yano, M., Hoogenraad, N.J. and Ryan, M.T. (2005) Dissection of the mitochondrial import and assembly pathway for human Tom40. *J. Biol. Chem.*, **280**, 11535–11543.
89. Rapaport, D. and Neupert, W. (1999) Biogenesis of Tom40, core component of the TOM complex of mitochondria. *J. Cell Biol.*, **146**, 321–331.
90. Dulloo, A.G. and Samec, S. (2001) Uncoupling proteins: their roles in adaptive thermogenesis and substrate metabolism reconsidered. *Br. J. Nutr.*, **86**, 123–139.
91. Strauss, J.F. III, Kishida, T., Christenson, L.K., Fujimoto, T. and Hiroi, H. (2003) START domain proteins and the intracellular trafficking of cholesterol in steroidogenic cells. *Mol. Cell. Endocrinol.*, **202**, 59–65.
92. Vonsattel, J.P., Myers, R.H., Stevens, T.J., Ferrante, R.J., Bird, E.D. and Richardson, E.P. Jr (1985) Neuropathological classification of Huntington's disease. *J. Neuropathol. Exp. Neurol.*, **44**, 559–577.
93. Vonsattel, J.P., Aizawa, H., Ge, P., DiFiglia, M., McKee, A.C., MacDonald, M., Gusella, J.F., Landwehrmeyer, G.B., Bird, E.D., Richardson, E.P. Jr *et al.* (1995) An improved approach to prepare human brains for research. *J. Neuropathol. Exp. Neurol.*, **54**, 42–56.